EUROPEAN ORGANIZATION FOR NUCLEAR RESEARCH

CERN-EP/84-16
15 February 1984

DRELL-YAN EVENTS FROM 400 GeV/c PROTONS : DETERMINATION OF THE K - FACTOR IN A LARGE KINEMATICAL DOMAIN

NA3 COLLABORATION

J. Badier[4], J. Boucrot[5], J. Bourotte[4], G. Burgun[1], O. Callot[5],
Ph. Charpentier[1], M. Crozon[3], D.Decamp[5], P. Delpierre[3], B. Gandois[1],
R. Hagelberg[2], M. Hansroul[2], Y. Karyotakis[4], W. Kienzle[2], P. Le Dû[1],
J. Lefrançois[5],Th. Leray[3][a], J. Maillard[3], A. Michelini[2], Ph. Miné[4],
G. Rahal[1][b], O. Runolfsson[2], P. Siegrist[1], A. Tilquin[3],.
R. Vanderhaghen[4], S. Weisz[4]

CEN,Saclay[1]-CERN,Geneva[2]-Collège de France,Paris[3]-
Ecole Polytechnique,Palaiseau[4]-Laboratoire de l'Accélérateur Linéaire,Orsay[5].

ABSTRACT

We present the analysis of ∿ 30 000 high mass dimuons ($M_{\mu\mu} > 4.5$ GeV/c) produced in 400 GeV/c proton-platinum interactions. A determination of the K - factor is given for different values of x_F and $M_{\mu\mu}$, and its variations are compared to QCD predictions. The proton structure functions derived from these events are compared to the values obtained in deep inelastic lepton scattering.

---

a) now at "Agence Française pour la maîtrise de l'Energie", Paris
b) now at CERN, Geneva

Submitted to Physics Letters B

Hadronic production of high mass lepton pairs (above the J/ψ meson) has been intensively studied since several years, mainly in relation with the large corrections, predicted by QCD, to the Drell-Yan parton model. However up to now all measurements from proton-proton or proton-nucleus interactions have been done either with high statistics but very limited acceptance [1], or with a large acceptance but limited statistics [2,3]. We present in this letter the analysis of a large sample (∿ 30 000) of high mass dimuon events coming from proton-platinum interactions at 400 GeV/c. These events were collected in the NA3 spectrometer at CERN, with a large acceptance to allow the first measurement of the "K-factor" over a large kinematical range : $4.5 \leqslant M_{\mu\mu} \leqslant 8.5$ GeV/c² and $x_F > 0$.

EXPERIMENTAL SET-UP

The NA3 spectrometer at CERN SPS has already been described [4] in its standard dimuon configuration corresponding to all previously published results. Some substantial modifications have been performed to take the data described in this letter :

i) The beam : to obtain high statistics, we have used a primary SPS proton beam at 400 GeV/c with an intensity around 1.5 10^9 protons per pulse. This intensity was about 30 times higher than for the pion beam used in previous data taking. In addition to the standard flux measurement using ionisation chambers, we have used activation measurements of Al and Cu foils. The two methods agree within 10% on the measured beam flux.

ii) The hadron filter length was increased from 1.5 to 3.2 m, in order to cope with the much larger intensity of the incoming beam. The central tungsten plug was conical with a 20 mrad aperture, and the target-dump distance was enlarged to 50 cm to give a good off-line separation of events coming from the target. The resulting hadronic punch-through and neutron background behind the large dump was comparable to that obtained in the previous data with 5 10^7 pions/pulse.

iii) The spectrometer : due to the length of the absorber, only one set of 6 MWPC planes was kept in front of the dipole magnet. The resulting momentum resolution on charged tracks was $\Delta p/p = 5\ 10^{-4} p$ (p in GeV/c).

iv) The trigger was modified in order to eliminate most of the low mass dimuons, which at such intensity would have saturated the data acquisition. A first requirement was the presence of at least 2 muons with $P_{Tv} > 1$ GeV (P_{Tv} being the vertical component of the transverse momentum), one in the upper and the other in the lower part of the spectrometer. A second condition was performed by a hardware processor, the "mass matrix", specially built to take the data presented here. The processor has been described in [5]; its purpose is to estimate the invariant mass of the dimuon from the relation :

$$M^2 \sim P_1 P_2 \theta^2 = \left(\frac{P_{Tv_1}}{\theta_{v_1}} + \Delta p\right)\left(\frac{P_{Tv_2}}{\theta_{v_2}} + \Delta p\right)\frac{(\theta_{v_1} + \theta_{v_2})^2}{\cos^2 \varphi}$$

where Δp is the energy loss of one muon in the hadron filter, the other quantities being defined in Fig. 1a.

The processor rejects about 90% of the triggers which remain after the selection on P_{Tv}. Fig. 1b gives the efficiency of the trigger as a function of the dimuon mass; about 80% of J/ψ mesons are rejected at the trigger level, without any loss above $M_{\mu\mu} = 5$ GeV/c².

It should be noticed that the response time of the "mass matrix" is about 170 ns and that 80% of events written on tape were fully reconstructed dimuons or multimuons.

RESULTS

We have collected $\sim$ 30 000 Drell-Yan events with $4.5 \leq M_{\mu\mu} \leq 8.5$ GeV/c² and with $x_F > 0$, from $8.25 \pm 0.8\ 10^{13}$ protons hitting a 6 cm thick Platinum target. This represents an integrated luminosity of $4.0 \pm 0.6\ 10^{39}$ cm^{-2}.

The acceptance of the apparatus has been computed using the method described in [6]. Drell-Yan events have been generated assuming a $1 + \cos^2 \theta^*$ angular distribution, and a nucleon sea structure function following the requirements $\bar{u}(x) = \bar{d}(x) = 2\bar{s}(x)$ and $\bar{c}(x) = 0$ (negligible charmed quarks contribution to the nucleon sea). The Fermi motion of the nucleons in the Platinum target has been taken as a simple Fermi gas with maximum momentum of 0.24 GeV/c. Following the measurements of ref.[1], the cross section dependence on the atomic number of the target is taken linear. We give in Tables I and II the differential cross-section $d^2\sigma/dx\,dM$, with statistical errors only; a global systematic error around 12% should be added to take into account the uncertainty on the luminosity measurement (beam flux measurements and effective number of nucleons in the target). The cross sections found in this experiment are in excellent agreement with the measurements of ref. [1] in the kinematical region where both experiments have a good acceptance.

COMPARISON WITH THEORETICAL PREDICTIONS

Proton-nucleon data can be easily compared to theoretical calculations, since the predicted cross section depends only on the nucleon structure functions which are measured in deep inelastic lepton scattering (D.I.S.) experiments. We take as input the most recent determination of the nucleon structure function from the CDHS experiment [7]

$$\begin{aligned} u_v(x) &= \frac{2}{B_u}\, x^{\alpha_1} (1-x)^{\beta_v} (1+\gamma x^{\alpha_2}) \\ d_v(x) &= \frac{1}{B_d}\, x^{\alpha_1} (1-x)^{\beta_v+1} (1+\gamma x^{\alpha_2}) \\ s(x) &= C(1-x)^{\beta_s} \end{aligned} \qquad (1)$$

with

$\alpha_1 = 0.3543 + 0.4122s$ $\qquad \alpha_2 = 1.576 + 2.017s$

$\beta_v = 3.833 + 2.868s$ $\qquad \gamma = 11.571$

$\beta_s = 7.4172 - 1.138s + 13.22s^2 - 4.9656s^3 - 1.8588s^4$

$C = (0.50758 + 0.23006s - 0.067345s^2)/2.8$

$s = \ln(\ln(Q^2/\Lambda^2)/\ln(5/\Lambda^2))$

$\Lambda = 0.3\ \mathrm{GeV/c^2}$

B_u and B_d are normalization factors which ensure that u_v and d_v obey the Gross-Llewellyn Smith sum rules

$$\left(\int_0^1 \frac{u_v(x)}{x}\,dx = 2 \quad \text{and} \quad \int_0^1 \frac{d_v(x)}{x}\,dx = 1\right);$$

the sea structure function s(x) corresponds to about 11% of the proton momentum carried by sea quarks at $Q^2 = 30/\mathrm{GeV}^2$.

This parametrization gives the predictions shown as dashed lines on Fig. 2; these predictions have to be scaled by a factor K in order to reproduce the data (full line on Fig. 2), with the usual definition :

$$K = \sigma_{\mathrm{experimental}}/\sigma_{\mathrm{predicted}} \text{ (leading log approximation)}$$

Table III gives the numerical values of K found in the present data for 4 bins in x_F and 4 bins in the dimuon mass. The variation of K with respect to x_F and M may be compared to next-to-leading log calculations in QCD [8]. In our kinematical range,K is predicted to be mass independent, and slowly decreasing as x_F increases (Fig. 3). Within the experimental errors, the observed variations (Fig. 2) of the K factor with respect to x_F are compatible with QCD predictions. The slight discrepancy observed on the M dependence cannot be an indication of different scaling violations in Drell-Yan and in Deep Inelastic Scattering, but rather reflects the dependence of the result on the choosen sea quark function.

The numerical values of K given in Table III are substantially higher than previously published [2, 3]. This can be explained by the fact that different parametrizations of the nucleon structure functions can change considerably the normalization. In particular it may be noticed that the fraction of momentum carried by sea quarks is taken in the present analysis to be 11% from Eq. (1), instead of 15% in ref. [3]. This problem on the value of the K factor was already discussed in detail in ref. [9] : it is shown for instance that the results of the CFS collaboration (ref. [1], where no K factor is estimated) give K = 2.4 if considered with a symmetric nucleon sea, and K = 3.5 if $\bar{u}(x) = \bar{d}(x)\ (1 - x)^{3.5}$ (asymmetric sea published by the CFS data).

DETERMINATION OF THE NUCLEON STRUCTURE FUNCTIONS

The expected variations of the K factor in our experimental range being predicted to be rather small, we can assume K = constant and try to extract from our data the nucleon structure function. We have chosen a Buras - Gaemers [10] parametrization :

$$u(x) = A\,x^{\alpha}(1-x)^{\beta v}$$
$$s(x) = C(1-x)^{\beta s}$$

and we obtain from our data :

$$\alpha = 0.60 \pm 0.08 \qquad (2)$$
$$\beta_v = 3.59 \pm 0.14$$
$$\beta_s = 9.03 \pm 0.30$$

Although this result has been obtained from a maximum likelihood - which is insensitive to the normalization constants A and C - we have computed the chisquare of the fit : $\chi^2 = 311$ for 294 degrees of freedom. Thus these simple functions give a good description of the shape of the nucleon structure function, with a small statistical error due to our high statistics in the domain $x > 0.2$, $< Q^2 > = 25$ GeV/c².

It must be noticed that the absolute normalization of the structure function cannot be presently measured. This experiment does not have experimental points below $x_1 = 0.2$ and thus measures only about 20% of the integral

$$\int_0^1 \frac{u(x)}{x}\,dx$$

The best available data from D.I.S. experiments do not have points below $x = 0.05$ (CDHS experiment) at the same Q^2, and measure only 50% of the above integral.

However, we can give a determination of the Drell-Yan K factor - considered as a constant over the kinematical range, which corresponds exactly to the definition given by theory. For that purpose we need to fix the normalization coefficients A and C in (2).

A has been determined from the following condition : the number of valence quarks between x = 0.2 and x = 1 must be the same for our fit and for the fit of D.I.S. experiment :

$$A \int_{0.2}^{1} \frac{u(x)}{x}\, dx = \frac{2}{B_u} \int_{0.2}^{1} x^{\alpha_1 - 1} (1 - x)^{\beta_V} (1 + \gamma x^{\alpha_2})\, dx$$

where u(x) is given in (2) and α_1, α_2, β_V, γ, Bu in (1). C has been determined from the condition that the momentum fraction carried by sea quarks has to be the same in both experiments.

With these normalizations we can extract a mean K factor in the kinematical range $0.2 \leq x \leq 1$ and $< Q^2 > = 25$ GeV^2.

K = 3.1 ± 0.5 (syst. NA3) ± 0.3 (syst. D.I.S.)

CONCLUSIONS

From this high statistics and large acceptance measurement of Drell-Yan events with incident 400 GeV/c protons, we may conclude :

i) We have measured the K-factor from Drell-Yan events induced by 400 GeV/c protons, in the kinematical domain $x_F > 0.$ and $4.5 \leq M_{\mu\mu} \leq 8.5$ GeV/c^2. The experimental variations of the K factor with x_F and $M_{\mu\mu}$ have been found very small. The absolute value is however significantly larger than predicted by next-to-leading log calculations in QCD. More precise predictions on higher order corrections are needed in order to allow a final comparison with our results.

ii) From a measurement which is completely independent of Deep Inelastic Experiments, we obtain a nucleon valence structure function which has the same shape in the common (x, Q^2) domain. This is in favour of the generally accepted assumption that the same structure functions can be used in Deep Inelastic Scattering and in Drell-Yan mechanisms.

ACKNOWLEDGEMENTS

It is a pleasure to thank the SPS staff, in particular N. Doble for the efficient tuning of the 400 GeV/c primary proton beam. We would like to thank the NA3 technical staff, in particular R. Lorenzi for the beam dump design and C. Lamy for her invaluable help in the processing of the data.

REFERENCES

[1] A.S. Ito et al., Phys. Rev. 23D (1981) 604.

[2] J. Badier et al., Phys. Lett. 89B (1979) 145, Phys. Lett. 96B (1980) 422.

[3] D. Antreasyan et al., Phys. Rev. Lett. 48 (1982) 302

[4] J. Badier et al., Nucl. Instr. and Meth. 175 (1980) 319.

[5] J. Boucrot et al., Nucl. Inst. and Meth. 174 (1980) 379.

[6] J. Badier et al., Zeitschrift für Physik C 18 (1983) 281.

[7] M. Abramowicz et al., Zeit. für Physik C 17 (1983) 283 and F. Eisele, private communication.

[8] J. Kubar et al., Nucl. Phys. B175 (1980) 251.

[9] F. Eisele, Rapporteur's talk, Proc. of the 21st Int. Conf. on High Energy Physics, Paris 1982, p C3-337. Les Editions de Physique, P. Petian and M. Porneuf, editors.

[10] A.J. Buras and K.J.F. Gaemers, Nucl. Phys. B132 (1978) 249.

TABLE CAPTIONS

Table 1 Differential cross section $d^2\sigma/dx_F dM$ in cm^2 for dimuon production on nucleons at 400 GeV/c within our acceptance, for $\Delta M = 0.2$ GeV/c^2, $\Delta x_F = 0.05$ cells

Table 2 Same as Table 1 for cells $\Delta M = 0.8$ GeV/c^2, $\Delta x_F = 0.2$

Table 3 Numerical values of the K factor obtained with parametrization (1) of the nucleon structure function (see text), for cells $\Delta M = 0.8$, $\Delta x = 0.2$

FIGURE CAPTIONS

Fig. 1 a) Definition of the kinematical variables used to take on-line estimation of the dimuon invariant mass.

b) Efficiency of the hardware processor selecting high mass dimuon events.

Fig. 2 Comparison between the data and the "leading log" approximation of the Drell-Yan cross section

a) x_F distributions

b) mass distributions

Dashed line : prediction of leading log approximation with the parametrization described in the text.

Full line : same parametrization, scaled by K factor.

Fig. 3 Theoretical predictions of the K factor variations with respect to x_F and M, from ref. [8].

Table I

MASS XF	.025		.075		.125		.175		.225	
	$d\sigma/dX_F\,dM$	$\Delta\sigma$								
4.6	.13E-33	.68E-35	.11E-33	.56E-35	.11E-33	.55E-35	.95E-34	.46E-35	.87E-34	.45E-35
4.8	.98E-34	.57E-35	.89E-34	.48E-35	.84E-34	.44E-35	.77E-34	.41E-35	.71E-34	.39E-35
5.0	.78E-34	.51E-35	.67E-34	.40E-35	.73E-34	.41E-35	.58E-34	.33E-35	.48E-34	.29E-35
5.2	.62E-34	.45E-35	.49E-34	.34E-35	.48E-34	.32E-35	.48E-34	.30E-35	.44E-34	.29E-35
5.4	.43E-34	.34E-35	.42E-34	.31E-35	.39E-34	.28E-35	.37E-34	.26E-35	.36E-34	.27E-35
5.6	.36E-34	.32E-35	.29E-34	.25E-35	.28E-34	.23E-35	.29E-34	.22E-35	.28E-34	.22E-35
5.8	.28E-34	.28E-35	.27E-34	.25E-35	.25E-34	.21E-35	.22E-34	.19E-35	.25E-34	.21E-35
6.0	.22E-34	.24E-35	.21E-34	.21E-35	.21E-34	.20E-35	.18E-34	.17E-35	.16E-34	.16E-35
6.2	.19E-34	.23E-35	.17E-34	.19E-35	.16E-34	.17E-35	.15E-34	.16E-35	.16E-34	.17E-35
6.4	.12E-34	.17E-35	.13E-34	.16E-35	.11E-34	.13E-35	.11E-34	.13E-35	.14E-34	.16E-35
6.6	.10E-34	.16E-35	.91E-35	.13E-35	.12E-34	.15E-35	.90E-35	.11E-35	.89E-35	.11E-35
6.8	.82E-35	.14E-35	.75E-35	.12E-35	.92E-35	.13E-35	.80E-35	.11E-35	.70E-35	.10E-35
7.0	.53E-35	.11E-35	.92E-35	.15E-35	.53E-35	.91E-36	.58E-35	.91E-36	.79E-35	.13E-35
7.2	.52E-35	.12E-35	.72E-35	.13E-35	.59E-35	.11E-35	.61E-35	.11E-35	.52E-35	.90E-36
7.4	.41E-35	.11E-35	.36E-35	.81E-36	.37E-35	.76E-36	.45E-35	.91E-36	.35E-35	.68E-36
7.6	.24E-35	.69E-36	.35E-35	.82E-36	.47E-35	.10E-35	.32E-35	.73E-36	.43E-35	.87E-36
7.8	.55E-35	.14E-35	.40E-35	.99E-36	.28E-35	.67E-36	.21E-35	.52E-36	.20E-35	.55E-36
8.0	.39E-35	.11E-35	.23E-35	.62E-36	.29E-35	.75E-36	.21E-35	.57E-36	.21E-35	.54E-36
8.2	.36E-35	.12E-35			.20E-35	.72E-36	.34E-35	.87E-36	.13E-35	.39E-36
8.4			.24E-35	.85E-36	.18E-35	.58E-36	.22E-35	.65E-36	.18E-35	.59E-36

XF	.275		.325		.375		.425		.475	
4.6	.81E-34	.46E-35	.59E-34	.38E-35	.45E-34	.33E-35	.42E-34	.37E-35	.28E-34	.29E-35
4.8	.66E-34	.40E-35	.48E-34	.32E-35	.41E-34	.31E-35	.34E-34	.31E-35	.20E-34	.24E-35
5.0	.50E-34	.33E-35	.40E-34	.29E-35	.35E-34	.29E-35	.26E-34	.25E-35	.17E-34	.20E-35
5.2	.41E-34	.29E-35	.31E-34	.25E-35	.24E-34	.21E-35	.18E-34	.20E-35	.14E-34	.17E-35
5.4	.32E-34	.25E-35	.22E-34	.19E-35	.18E-34	.18E-35	.18E-34	.20E-35	.14E-34	.18E-35
5.6	.23E-34	.20E-35	.21E-34	.19E-35	.18E-34	.19E-35	.16E-34	.20E-35	.13E-34	.18E-35
5.8	.21E-34	.20E-35	.18E-34	.19E-35	.13E-34	.15E-35	.13E-34	.16E-35	.90E-35	.15E-35
6.0	.16E-34	.16E-35	.13E-34	.15E-35	.12E-34	.14E-35	.92E-35	.13E-35	.72E-35	.13E-35
6.2	.13E-34	.14E-35	.13E-34	.15E-35	.89E-35	.12E-35	.69E-35	.11E-35	.51E-35	.94E-36
6.4	.11E-34	.13E-35	.11E-34	.14E-35	.68E-35	.10E-35	.55E-35	.95E-36	.43E-35	.86E-36
6.6	.90E-35	.12E-35	.86E-35	.12E-35	.60E-35	.10E-35	.52E-35	.96E-36	.30E-35	.67E-36
6.8	.68E-35	.10E-35	.60E-35	.95E-36	.48E-35	.82E-36	.39E-35	.78E-36	.38E-35	.86E-36
7.0	.47E-35	.81E-36	.45E-35	.81E-36	.49E-35	.89E-36	.22E-35	.51E-36	.28E-35	.77E-36
7.2	.55E-35	.97E-36	.33E-35	.66E-36	.29E-35	.63E-36	.35E-35	.80E-36	.22E-35	.59E-36
7.4	.51E-35	.10E-35	.44E-35	.95E-36	.20E-35	.50E-36	.22E-35	.58E-36	.22E-35	.65E-36
7.6	.45E-35	.93E-36	.23E-35	.55E-36	.23E-35	.58E-36	.19E-35	.52E-36	.25E-35	.84E-36
7.8	.22E-35	.58E-36	.23E-35	.58E-36	.18E-35	.50E-36	.21E-35	.62E-36	.10E-35	.39E-36
8.0	.23E-35	.67E-36	.22E-35	.58E-36	.22E-35	.71E-36	.23E-35	.71E-36	.53E-36	.22E-36
8.2	.19E-35	.54E-36	.19E-35	.51E-36	.19E-35	.63E-36				
8.4	.14E-35	.45E-36	.16E-35	.52E-36	.16E-35	.52E-36				

XF	.525		.575		.625	
4.6	.17E-34	.24E-35	.12E-34	.23E-35	.75E-35	.21E-35
4.8	.19E-34	.26E-35	.98E-35	.19E-35	.81E-35	.22E-35
5.0	.11E-34	.18E-35	.12E-34	.22E-35	.40E-35	.11E-35
5.2	.96E-35	.15E-35	.57E-35	.11E-35	.46E-35	.12E-35
5.4	.74E-35	.13E-35	.72E-35	.14E-35	.41E-35	.11E-35
5.6	.72E-35	.13E-35	.42E-35	.10E-35	.32E-35	.99E-36
5.8	.59E-35	.11E-35	.39E-35	.98E-36	.20E-35	.70E-36
6.0	.39E-35	.90E-36	.23E-35	.61E-36		
6.2	.45E-35	.98E-36	.46E-35	.12E-35		
6.4	.32E-35	.77E-36	.15E-35	.49E-36		
6.6	.39E-35	.95E-36	.12E-35	.43E-36		
6.8	.25E-35	.69E-36	.20E-35	.68E-36		
7.0	.15E-35	.43E-36	.22E-35	.83E-36		
7.2	.25E-35	.83E-36	.98E-36	.37E-36		
7.4	.22E-35	.79E-36				
7.6	.11E-35	.40E-36				
7.8	.94E-36	.40E-36				
8.0	.13E-35	.53E-36				
8.2						
8.4						

Table II

MASS XF	.100		.300		.500		.700		.900	
	$d\sigma/dX_F\,dM$	$\Delta\sigma$								
4.9	.79E-34	.11E-35	.51E-34	.83E-36	.18E-34	.57E-36	.29E-35	.31E-36	.14E-36	.79E-37
5.7	.29E-34	.61E-36	.21E-34	.48E-36	.88E-35	.35E-36	.13E-35	.16E-36		
6.5	.12E-34	.37E-36	.93E-35	.31E-36	.38E-35	.21E-36	.61E-36	.91E-37		
7.3	.49E-35	.25E-36	.41E-35	.20E-36	.19E-35	.14E-36	.24E-36	.51E-37		
8.1	.26E-35	.18E-36	.19E-35	.14E-36	.86E-36	.91E-37	.17E-36	.40E-37		

X_F	0.0		0.2		0.4		0.6	0.8
M	K	ΔK	K	ΔK	K	ΔK	K	ΔK
7.7								
	3.51	.18	3.46	.17	3.79	.30	3.56	.93
6.9								
	3.19	.10	3.13	.10	3.04	.17	4.07	.71
6.1								
	3.01	.07	2.82	.07	2.91	.12	3.08	.38
5.3								
	3.05	.04	2.74	.05	2.50	.08	2.54	.31
4.5								

Table III

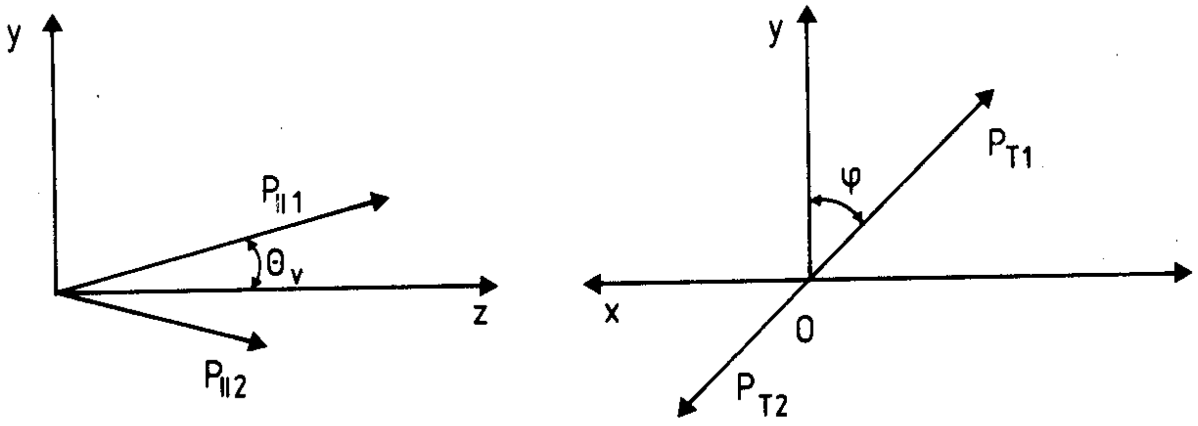
y
$P_{\parallel 1}$
θ_v
z
$P_{\parallel 2}$
y
P_{T1}
φ
x
0
P_{T2}

FIG. 1a

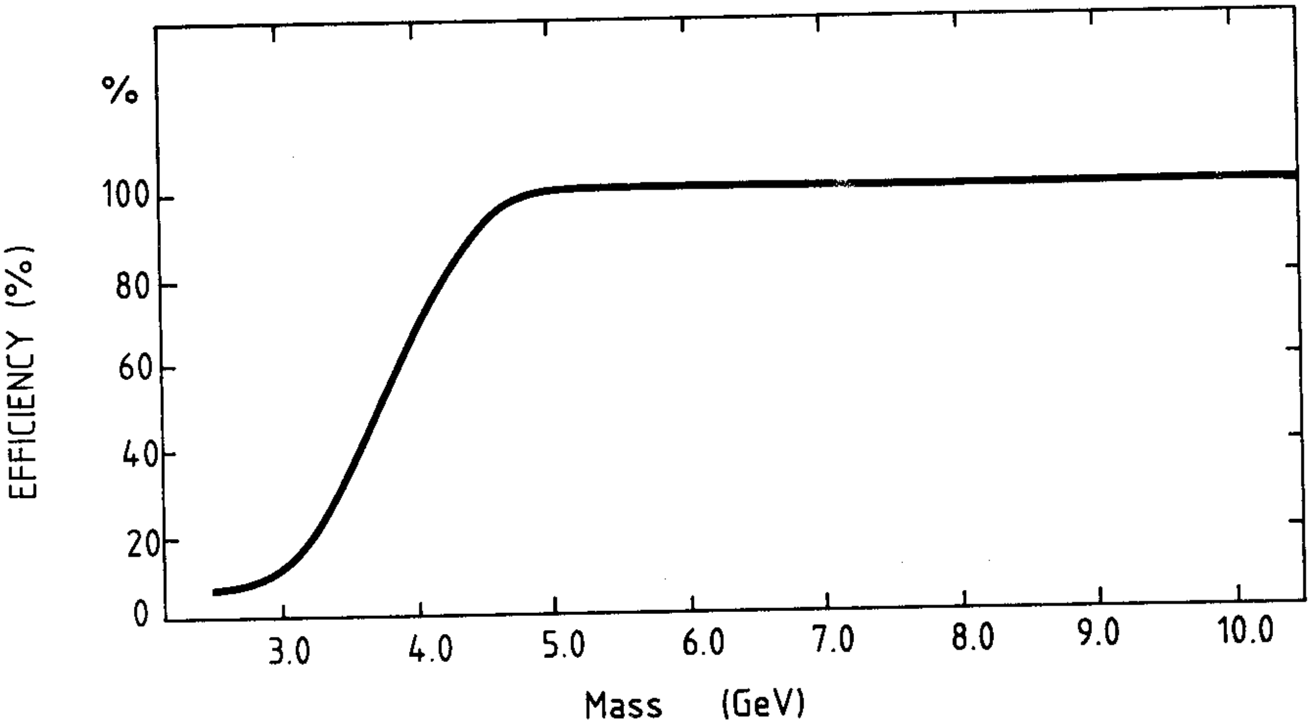
%
100
80
60
40
20
0
EFFICIENCY (%)
3.0
4.0
5.0
6.0
7.0
8.0
9.0
10.0
Mass (GeV)

FIG. 1b

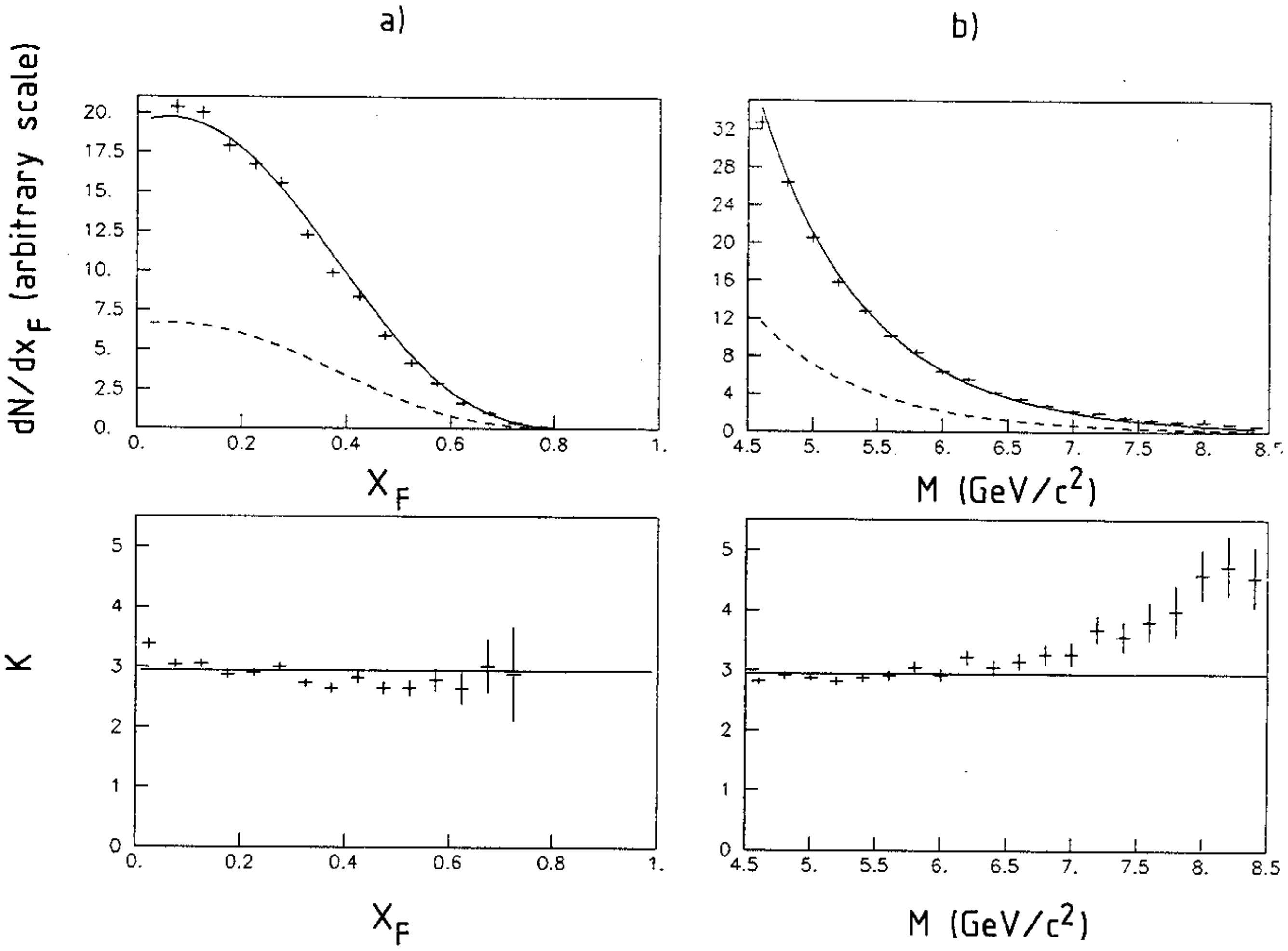
a)
b)
dN/dx_F (arbitrary scale)
20.
17.5
15.
12.5
10.
7.5
5.
2.5
0.
0.2
0.4
0.6
0.8
1.
X_F
32
28
24
20
16
12
8
4
0
4.5
5.
5.5
6.
6.5
7.
7.5
8.
8.5
M (GeV/c²)
K
5
4
3
2
1
0
X_F
M (GeV/c²)

FIG. 2

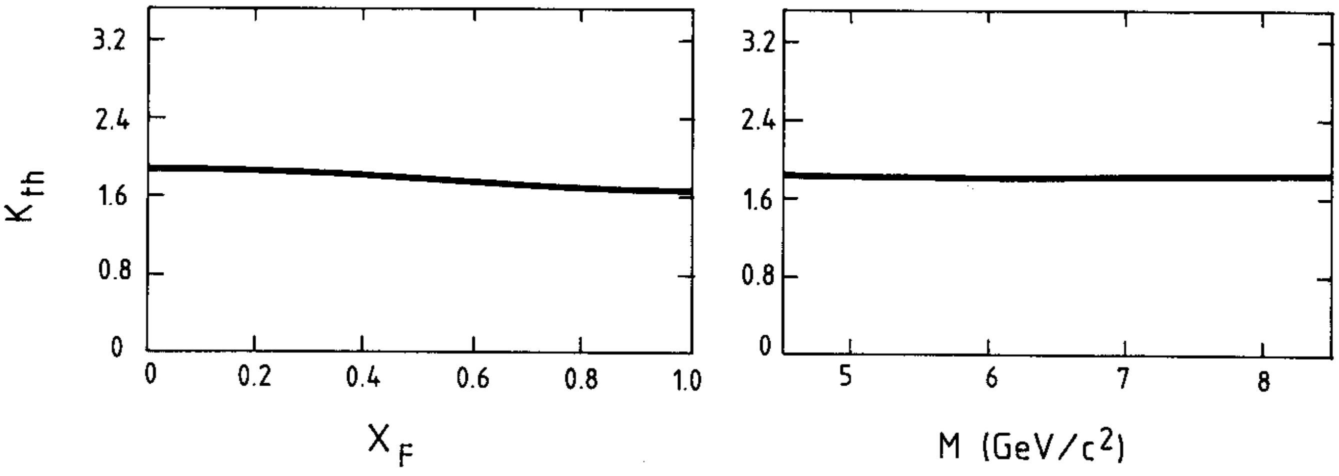
K_th
3.2
2.4
1.6
0.8
0
0.2
0.4
0.6
0.8
1.0
X_F
5
6
7
8
M (GeV/c²)

FIG. 3